Biosorption of Trivalent Chromium on the Brown Seaweed Biomass

YEOUNG-SANG YUN,[†] DONGHEE PARK,[‡]
JONG MOON PARK,*,[‡] AND
BOHUMIL VOLESKY[†]

*Department of Chemical Engineering,
School of Environmental Science and Engineering,
Pohang University of Science and Technology,
San 31, Hyoja-dong, Pohang 790-784, Korea, and
Department of Chemical Engineering, McGill University,
3610 University Street, Montreal, Quebec H3A 2B2, Canada*

Biosorption has attracted attention as a cost-effective means for the treatment of metal-bearing wastewater. However, the mechanism of metal binding is not clearly understood, and consequently, modeling of the biosorption performance is still raising debates. In this study, the biosorption of trivalent chromium was investigated with protonated brown alga *Ecklonia* biomass as a model system. Titration of the biomass revealed that it contains at least three types of functional groups. The Fourier transform infrared spectrometry showed that the carboxyl group was the chromium-binding site within the pH range (pH 1–5) used in this study, where chromium does not precipitate. The pK value and the number of carboxyl groups were estimated to be 4.6 ± 0.1 and 2.2 ± 0.1 mmol/g, respectively. The equilibrium sorption isotherms determined at different solution pH indicated that the uptake of chromium increased significantly with increasing pH. A model for the description of chromium biosorption was developed incorporating the hydrolysis reactions that chromium undergoes in the aquatic phase. The model was able to predict the equilibrium sorption experimental data at different pH values and chromium concentrations. In addition, the speciation of the binding site as a function of the solution pH was predicted using the model in order to visualize the distribution of chromium ionic species on the binding site.

Introduction

Chromium is generally found in electroplating and metal-finishing industrial effluents, sewage and wastewater treatment plant discharge, and cooling water that often contains chromate additive (*1*). Among the several oxidation states (di-, tri-, penta-, and hexa-), trivalent chromium together with the hexavalent state can be mainly present in the aquatic environment (*2*). Although trivalent chromium is less toxic than hexavalent chromium, a long-term exposure to trivalent chromium is known to cause allergic skin reactions and cancer (*3*). As a result, the total chromium level in the effluent is strictly regulated in many countries.

Currently, chemical precipitation is most widely used for the treatment of chromium-bearing effluents (*4*). However, a major disadvantage of this method is the undesirable production of significant amounts of chemical sludge. Ion-exchange treatment can minimize the sludge generation, but the high cost of resins has limited its wide application for wastewater treatment.

Recently, it has been confirmed that various biosorbents are able to effectively remove chromium (*4–11*). Some of the biomass types have a comparable (or even superior) sorption performance to synthetic ion-exchange resins (*5, 9*). The living bacterium *Sphaerotilus natans* was especially reported to accumulate as much as 120 mg of chromium/g of biomass (*5*). In general, however, it is neither easy nor cheap to maintain a dominant microbial culture in the chromium-bearing effluents. Accordingly, there has been an extensive search for practically useful biomass, in its nonliving state, capable of effectively removing chromium (*4, 6–11*). Researchers have tested such types of dead biomass as yeasts (*6*), milled peat (*7*), microalgae (*8*), fungi (*9*), and seaweed (*4, 11*) for their ability to sequester chromium. Unlike microorganisms, the size of seaweed biomass is large enough to facilitate its application without a cumbersome solid–liquid separation process. For this reason, the seaweed biomass has been used for biosorption research and has been confirmed to be a good biosorbent for removal of various heavy metal ions, such as gold, cadmium, copper, zinc, etc. (*12*). Furthermore, many kinds of seaweed proliferate ubiquitously and abundantly in the littoral zones of the world's oceans, making the seaweed biomass readily available and inexpensive.

Although extensive studies on chromium biosorption (*4–11*) have been carried out, its biosorption performance has not been modeled. In the previous studies, empirical models such as the Langmuir or Freundlich equations were used in order to quantitatively evaluate the chromium uptake of different biosorbents. However, such empirical models are invariably not sensitive to different biosorption mechanisms and cannot predict the biosorption performance depending on pH, ionic strength, and other environmental variables. Furthermore, the binding sites for chromium have not been specifically identified, which is a prerequisite for more advanced modeling attempts.

In this study, biosorption of trivalent chromium by the abundant low-cost seaweed biomass (*Ecklonia* sp.) was investigated. The functional groups for chromium biosorption were identified whereby the chromium binding to the functional group was mathematically modeled based upon the ion-exchange mechanism, reflecting also chromium hydrolysis reactions in the aqueous phase.

Materials and Methods

Preparation of the Biomass. The brown seaweed *Ecklonia* sp. was collected along the seashore of Pohang, Korea. In the previous study (*11*), this seaweed biomass was successfully used for chromium removal from a tin-plating effluent. The sun-dried biomass was treated with a 2 N H_2SO_4 solution, replacing the natural mix of ionic species with protons. The acid-treated biomass, designated as protonated biomass in this paper, was washed with deionized distilled water several times and thereafter dried at 80 °C in an oven for 24 h. The resulting dried *Ecklonia* biomass was used as a biosorbent in the following experiments.

Potentiometric Titration of the Biomass. The potentiometric titration was carried out for two different concentrations of the biomass (5 and 1 g/L). Tens of 50-mL flasks were used for the titration experiments. First, the weighed biomass and 20 mL of deionized water (CO_2-free) were put into each flask. Here, CO_2-free water was obtained by

* Corresponding author e-mail: jmpark@postech.ac.kr; phone: +82-54-279-2275; fax: +82-54-279-2699.
† McGill University.
‡ Pohang University of Science and Technology.

stripping deionized water with nitrogen gas for 2 h with vigorous mixing. A different volume of 1 N HaOH or 1 N H_2SO_4 was added into each flask containing the biomass suspension. Flasks were agitated using a shaker (200 rpm) at room temperature for 24 h. Preliminary tests showed that 24 h was sufficient time for reaching the sorption equilibrium. Thereafter, the equilibrium pH was measured using an electrode (Ingold). During the titration experiments, the CO_2-free condition was always maintained to avoid the influence of inorganic carbon on the solution pH.

Sorption Dynamics Experiments. To determine the contact time required for the sorption equilibrium experiments, the sorption dynamics was examined first. The initial concentration of chromium was 100 mg/L, and the desired amount of biomass was added into the flask containing 200 mL of chromium solution. The flasks were agitated on a shaker at 200 rpm and room temperature. The solution pH was maintained at the desired value (pH 4.0 or 3.0) by using a 1 N NaOH solution.

Samples were intermittently removed from the flasks in order to analyze the chromium concentration following appropriate dilution. The total volume of withdrawn samples did not exceed 2% of the working volume (200 mL). The chromium stock solution was made by dissolving the analytical grade $CrCl_3 \cdot 6H_2O$ (Sigma).

Equilibrium Sorption Experiments. Two kinds of equilibrium sorption experiments were carried out: *isotherm* and *pH edge* experiments. In general, the isotherm represents the equilibrium relationship between the metal uptake by sorbent and the final metal concentration in the aqueous phase. On the other hand, the pH edge is an equilibrium plot of metal uptake versus final pH. The isotherm is powerful for evaluation of sorption capacity of the biosorbent; the sorption edge is helpful to understand the variability of sorption with the pH.

For the chromium biosorption isotherms, different initial Cr concentrations (0−500 mg of Cr/L) were prepared in a series of 125-mL Erlenmeyer flasks using chromium chloride solution (50 mL). Following the addition of biomass (0.25 g) into each flask, the suspension was agitated on the rotary shaker (200 rpm, room temperature), and the solution pH was maintained at the desired value using 1 N NaOH or 1 N H_2SO_4. The required contact time to reach sorption equilibrium was 24 h as determined in the sorption dynamic experiments. After the sorption system reached the equilibrium state, the samples were taken from the flasks and diluted properly with deionized water for analysis of chromium concentration. Detailed standard procedure for determination of the sorption isotherm has been reported elsewhere (*13*).

In the pH edge experiments, the initial concentration of chromium was identical (52 mg/L) in all flasks, unlike for the isotherm experiments. Furthermore, the pH was intentionally altered by means of adding 1 N NaOH or 1N H_2SO_4 into the flasks (it was constant in the isotherm experiments). Other conditions for the pH edge experiments were identical with those in the isotherm experiments. After 24 h, the equilibrium pH was measured, and the liquid samples were used for the analysis of chromium concentration.

In both isotherm and pH edge experiments, the chromium uptake (*q*) was calculated from the mass balance as follows:

$$q = \frac{[Cr]_i - [Cr]_f}{W/V} \tag{1}$$

where $[Cr]_i$ and $[Cr]_f$ are the initial and final concentrations of chromium; W and V are the biomass weight and the solution volume, respectively. The change of working volume due to additions of NaOH or H_2SO_4 was negligible in both types of experiments.
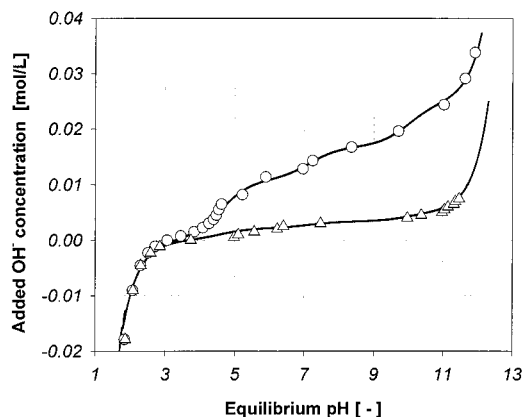
FIGURE 1. Potentiometric titration of the protonated *Ecklonia* biomass. The biomass concentrations are (○) 5 and (△) 1 g/L. The lines are produced by the titration model (eq 6).

Chromium Analysis. To analyze the chromium concentration, trivalent chromium was first converted into the hexavalent state by oxidation with potassium permanganate at a high temperature (130−140 °C) under acidic conditions. Thereafter, the chromium concentration was determined colorimetrically by the acidic reaction with 1,5-diphenylcarbazide. The absorbance of the resulting red-violet sample was measured at 540 nm using a spectrophotometer (Spectronic 21, Milton Roy Co.). The analytical method for chromium is detailed in Standard Methods (*14*).

Fourier Transform Infrared Analysis (FTIR). Infrared spectra of the protonated and chromium-loaded biomass were obtained using a Fourier transform infrared spectrometer (FTIR 1600, Perkin-Elmer). The FTIR study was also carried out with biomass stripped of chromium by desorbing it with 2 N H_2SO_4. For the FTIR study, 5 mg of finely ground biomass was encapsulated in 400 mg of KBr in order to prepare the translucent sample disks.

Results and Discussion

Characterization of Chromium Binding Sites. The biomass titration curve displays its distinct characteristics depending upon types and amounts of functional groups present in the biomass. The titration results of the protonated *Ecklonia* biomass are shown in Figure 1. When a higher concentration of biomass was used, the equilibrium pH was less dependent on the added hydroxide concentration due to the higher buffering capacity present in the system. In the case where 5 g/L of biomass was used, an inflection point can obviously be seen between pH 4 and pH 5, indicating the existence of a functional group with a pK_H value between 4 and 5. The buffer capacity extends over a much larger region than this; therefore, other functional groups must be present. However, their identities could not be definitely confirmed from the inflection points of the titration curves, their quantities being probably much smaller than that of the main functional group.

To evaluate the properties of functional groups quantitatively, we can consider the functional sites on the biomass. Considering a certain group (B_jH), its reaction with a proton and its related equilibrium constant (K_j) may be defined as follows:

$$B_jH \leftrightarrow B_j^- + H^+ \qquad K_j = \frac{[B_j^-][H^+]}{[B_jH]} \tag{2}$$
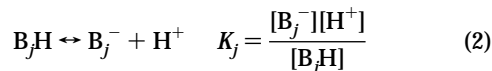
The total concentration ($[B_j]_T$) of the functional group is equal to the sum of the protonated and ionized configurations. The protonated group can be expressed using eq 2 as $[B_jH] = [B^-][H^+]/K_j$. Therefore

$$[B_j]_T = [B_jH] + [B_j^-] = [B_j^-]\left(1 + \frac{[H^+]}{K_j}\right) \quad (3)$$

Consequently, the concentration of the ionized group can be expressed as a function of the total concentration of the site and of the proton concentration:

$$[B^-] = \frac{[B_j]_T}{1 + [H^+]/K_j} \quad (4)$$

In the titration experiments, the electroneutrality condition must be satisfied. Therefore

$$[Na]_{added} + [H^+] = \sum_{j=1}^{N} [B_j^-] + [OH^-] \quad (5)$$

where $\sum_{j=1}^{N}[B_j^-]$ represents a sum of the concentrations of all types (1−Nth type) of ionized groups; $[Na]_{added}$ is identical to the concentration of added hydroxide ions. Combining eqs 4 and 5 yields

$$[Na]_{added} = \sum_{j=1}^{N} \frac{b_jX}{1 + [H^+]/K_j} + \frac{K_W}{[H^+]} - [H^+] \quad (6)$$

where b_j and X are represent the quantity of the specific functional groups per unit mass of biomass (mmol/g) and the biomass concentration, respectively. In this work, the change of the working volume due to addition of NaOH was compensated for during the data processing.

Equation 6 contains two parameters per one functional group: the equilibrium constant (K_j) and the amount of the functional group per weight (b_j). To examine the number of functional groups, the titration model (eq 6) was simultaneously fitted to all the titration curves (total 43 data points) obtained at two biomass concentrations. The nonlinear regression was performed by means of the Marquardt−Levenberg algorithm (15) using the technical software Mathematica 4.0 (16).

As a result, one or two functional groups were insufficient to describe the titration results (data not shown). Meanwhile, the three-site model was able to describe the entire titration curves (Figure 1). This indicated that the *Ecklonia* biomass has at least three types of organic functional groups. The estimated parameters are summarized in Table 1. The first site was established as the most abundant (2.2 ± 0.1 mmol/g). The negative logarithm of the equilibrium constant (pK_H) for proton binding to the first group was estimated to be 4.6 ± 0.1. Carboxyl groups in biological polymers have pK_H values ranging from 3.5 to 5.0 (17); therefore, the first group was believed to be the carboxyl group. A similar result was obtained for the brown seaweed *Sargassum* biomass, whereby its carboxyl group was shown to have a pK_H value of 4.5 (18). The last functional group seemed to be the hydroxyl (or phenolic) group that generally shows pK_H values between 9.5 and 10.5 depending on the structure of main chains (17). The second group (pK_H = 7.2 ± 0.4) could not be identified, not even approximately, because there are many kinds of functional groups (i.e., phosphoryl, amino, and imidazole group) of biological polymers that have the pK_H values covering 7.2 (17, 19).

To confirm the type of functional groups, the FTIR study was carried out. As shown in Figure 2, the FTIR spectrum of the protonated biomass displays a number of absorption peaks, indicating the complex nature of the biomass examined. The broad absorption peak around 3350 cm^{-1} is indicative of the existence of bonded hydroxyl group (3340−3380 cm^{-1}) (20, 21), which possibly has pK_H = 10.0 ± 0.3 as expected from the titration model. The peak observed at

TABLE 1. Dissociation Constants (K) and Contents (b) of Three Functional Groups in the *Ecklonia* Biomass[a]

functional groups	pK_H (−)	b (mmol/g)
1st (carboxyl) group	4.6 (0.1)	2.2 (0.2)
2nd (?) group	7.2 (0.4)	1.2 (0.3)
3rd (hydroxyl) group	10.0 (0.3)	1.6 (0.3)

[a] Standard errors are given in parentheses, and the coefficient of determination (R^2) of the nonlinear regression is 0.99.
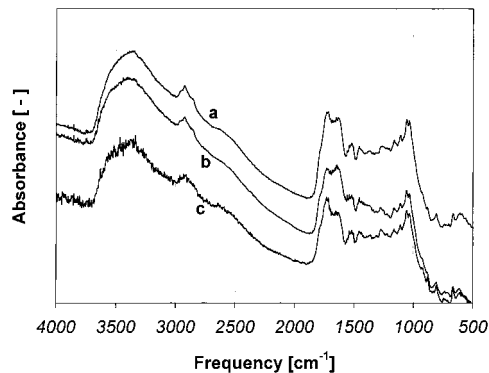
FIGURE 2. Fourier transform infrared absorption spectra of the *Ecklonia* biomass. Lines: (a) protonated biomass, (b) chromium-loaded biomass, (c) chromium-eluted biomass obtained by desorption of chromium-loaded biomass.

2924 cm^{-1} can be assigned to the CH group (21). The spectrum also displays the absorption peak at 1838 cm^{-1} corresponding to the stretching band of the free carboxyl double bond from the carboxyl functional group (22). The phosphate group shows some characteristic absorption peaks around 1150 cm^{-1} (P=O stretching), 1040−910 cm^{-1} (P−OH stretching), and 1050−970 cm^{-1} (P−O−C stretching) (23). The absorption peak around 850 cm^{-1} may correspond to the S=O bond, indicating the existence of the sulfonate group that is often found in the seaweed biomass (22).

The absorption spectrum of chromium-laden biomass (at pH 4) was compared with that of protonated biomass. Furthermore, an FTIR spectrum was also obtained for the chromium-loaded biomass after it was desorbed with 2 N H$_2$SO$_4$. The chromium-loaded and eluted biomass were washed, dried, and powdered under the same conditions used in the preparation of protonated biomass. A significant shift of absorption peaks can be seen when comparing the FTIR spectra of protonated and chromium-loaded biomass (Figure 2). The peak around 1740 cm^{-1} (C=O stretching) almost disappeared for the Cr-laden biomass, while the peak around 1630 cm^{-1} (C=O chelate stretching) became higher. After chromium was desorbed, the spectrum of chromium-eluted biomass became similar to that of protonated biomass. This reflects chromium binding to the carboxyl group. The carboxyl group is likely located in alginate, which is known to be a key component in the seaweed biomass for uptake of divalent metal ions such as cadmium, lead, and calcium (22, 24).

The titration and FTIR studies revealed several types of chemical groups in the biomass that are likely to participate in metal binding. Since trivalent chromium is precipitated as chromium hydroxide at pH > 5, the chromium biosorption experiments were carried out in the range of pH 1−5. In this pH range (pH < pK_{H2} < pK_{H3}), the second and third functional groups should be completely protonated. Therefore, it can be concluded that although all of three titrable sites are potentially capable of binding the chromium cation, only the carboxyl group could play a significant role in the chromium biosorption under the given experimental conditions.
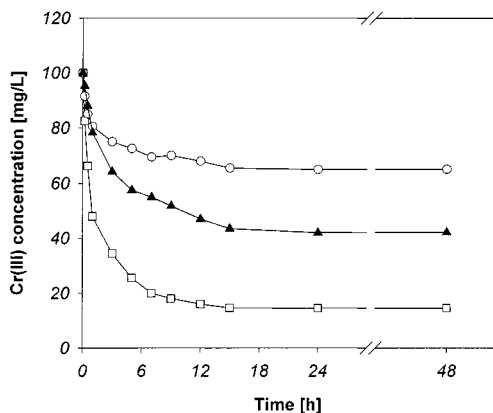
FIGURE 3. Dynamics of batch chromium biosorption at different pH values and biomass concentrations (X). Symbols: (□) pH 4.0 and $X = 5.0$ g/L; (○) pH 3.0 and $X = 5.0$ g/L; (▲) pH 4.0 and $X = 2.5$ g/L.
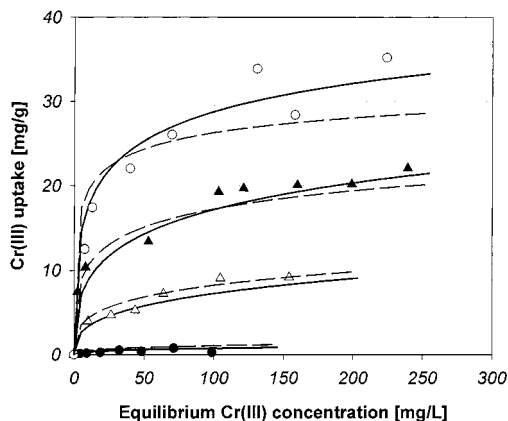
FIGURE 4. Chromium isotherms at different pH values. Experimental data: (●) pH 2.0; (△) pH 3.0; (▲) pH 3.5; (○) pH 4.0. The continuous lines were predicted by the model considering chromium hydrolysis (eq 14); the dotted lines were produced by the model not considering the chromium hydrolysis (eq 15).

Effect of pH on Chromium Uptake. The dynamics of chromium biosorption were studied in order to determine the contact time required for reaching the sorption equilibrium (Figure 3). The solution pH and biomass concentration affected the removal rate of chromium. The observed chromium biosorption proceeded up to approximately 95% within 12 h, and the equilibrium state could be reached after 24 h of contact time. This was used as a guide for the following biosorption equilibrium experiments.

Figure 4 shows the experimental chromium biosorption isotherms obtained at various pH values. The chromium uptake increased with increasing equilibrium concentrations and eventually reached a certain saturated value depending on the pH. Although empirical models such as the Langmuir equation cannot provide any mechanistic understanding of the sorption phenomena, the latter may be conveniently used to estimate the maximum uptake of chromium from experimental data. The Langmuir parameters were estimated using the nonlinear regression method and are summarized in Table 2. The maximum uptake (q_{max}) increased with increasing equilibrium pH. Since the carboxyl group has $pK_H = 4.6$, it can be easily expected that at a low pH these sites are occupied by protons, whereby chromium cannot become easily bound to the sites. At pH 4, the maximum Cr uptake was estimated to be 24.1 mg/g, corresponding to 1.97 mequiv/g, based on the assumption that chromium exists solely as Cr^{3+} at this pH. As a matter of fact, since $CrOH^{2+}$ is the dominant species (~74%) at pH 4 (Figure 5), the number of

TABLE 2. Estimated Langmuir Parameters at Different pH Values[a]

pH (—)	q_{max} (mg/g)	K (mg/L)	R^2 [c]
2.0[b]			
3.0	11.0 (1.3)	31.7 (11.4)	0.94
3.5	20.5 (1.1)	7.4 (2.8)	0.93
4.0	34.1 (1.8)	14.2 (3.2)	0.96

[a] Standard errors are given in parentheses. [b] At pH 2, the isotherm could not be described by the Langmuir model. [c] The R^2 values are the coefficients of determination.
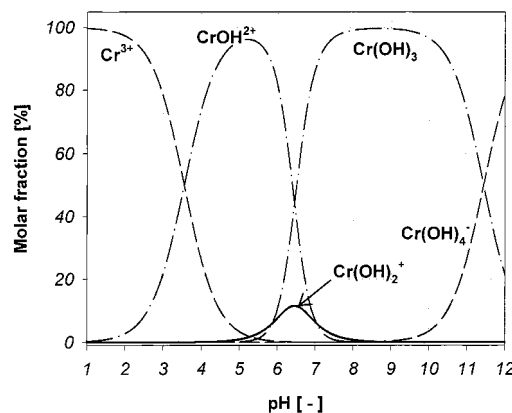
FIGURE 5. Chromium speciation depending on the pH. The curves were produced by using the thermodynamic data reported in the literature (27).

sites occupied by chromium (1.97 mequiv/g) must be overestimated. Nevertheless, it was even less than the total number of available sites (2.2 mequiv/g). This reflects the fact that the binding sites were not saturated with chromium but were either empty or occupied by protons. The speciation of the binding sites will be discussed quantitatively in the last part of Results and Discussion.

Modeling of Chromium Biosorption. For modeling the biosorption of heavy metal ions, the speciation of metals should be first examined because the metal speciation may affect the biosorption performance especially in cases where the valence of ions changes due to hydrolysis reactions (25). The speciation of chromium was calculated as a function of the pH (Figure 5) from thermodynamic data describing chromium hydrolysis (26). At pH >5, chromium begins to precipitate as $Cr(OH)_3$. In the range of pH $1-5$ studied in the present work, Cr^{3+} and $CrOH^{2+}$ are major species, whereby $Cr(OH)_2^+$ was found to be negligible. The fraction of aqueous chromium species is highly dependent upon the pH, and the two species can be equally present at pH 3.55. In this pH range, the speciation of chromium can be expressed by the following reaction:

$$Cr^{3+} + H_2O \leftrightarrow CrOH^{2+} + H^+$$

$$K_S = \frac{[CrOH^{2+}][H^+]}{[Cr^{3+}]} = 10^{-3.55} \quad (7)$$
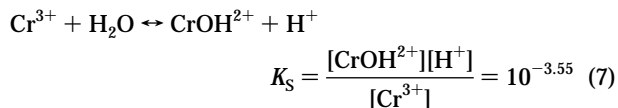
The biosorption of heavy metal ions, especially by seaweed biosorbents, has been elucidated to be mainly based on the ion-exchange phenomenon (27–29). Furthermore, the biosorption of trivalent chromium is qualitatively shown to be a cationic-exchange process (11) between chromium ions (Cr^{3+} and/or $CrOH^{2+}$) and protons of the biomass carboxyl groups, as previously indicated. The binding reactions and the corresponding equilibrium constants can be defined as follows:

$$3B^- + Cr^{3+} \leftrightarrow 3Cr_{1/3}B \quad K_{M1} = \frac{[Cr_{1/3}B]^3}{[B^-]^3[Cr^{3+}]} \quad (8)$$

$$2B^- + CrOH^{2+} \leftrightarrow 2(CrOH)_{1/2}B \quad K_{M2} = \frac{[(CrOH)_{1/2}B]^2}{[B^-]^2[CrOH^{2+}]} \quad (9)$$
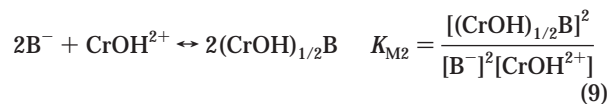
Here, the formulation of metal-binding sites was chosen as $3Cr_{1/3}B$ and $2(CrOH)_{1/2}B$ instead of CrB_2 and $CrOHB_2$, respectively, to emphasize that two or three bonds have to be broken in competitive binding or upon desorption of the metal (30).

When the biomass is reacted with the metal solution, the binding sites become occupied by Cr^{3+}, $CrOH^{2+}$, and protons, or the sites remain free. Therefore, the mass balance for the sites can be described as follows:

$$[B]_T = [B^-] + [BH] + [Cr_{1/3}B] + [(CrOH)_{1/2}B] \quad (10)$$

By substituting eqs 2, 8, and 9 into eq 10, the concentration of free sites can be expressed:

$$[B^-] = \frac{[B]_T}{1 + [H^+]/K_H + \sqrt[3]{K_{M1}[Cr^{3+}]} + \sqrt[2]{K_{M2}[CrOH^{2+}]}} \quad (11)$$

The chromium uptake can be calculated from the bound forms of the two chromium species as shown in eq 12. Furthermore, combining eqs 8 and 9 with eq 12 yields

$$qX = \frac{1}{3}[Cr_{1/3}B] + \frac{1}{2}[(CrOH)_{1/2}B] \quad (12)$$

$$q = \frac{b_T\left(\frac{1}{3}\sqrt[3]{K_{M1}[Cr^{3+}]} + \frac{1}{2}\sqrt[2]{K_{M2}[CrOH^{2+}]}\right)}{1 + [H^+]/K_H + \sqrt[3]{K_{M1}[Cr^{3+}]} + \sqrt[2]{K_{M2}[CrOH^{2+}]}} \quad (13)$$

Equation 13 contains the concentrations of the two chromium species. However, only the total trivalent chromium ($[Cr^{3+}]$ plus $[CrOH^{2+}]$) can be experimentally measured. Therefore, it is necessary to convert each species into a lumped term of the total concentration ($[Cr]_T$) using the speciation equilibrium relationship (eq 7). The resulting equilibrium uptake of chromium can be expressed as a function of concentrations of chromium and protons:

$$q = \frac{b_T\left(\frac{1}{3}\sqrt[3]{\dfrac{K_{M1}[Cr]_T}{1 + K_S/[H^+]}} + \frac{1}{2}\sqrt[2]{\dfrac{K_{M2}[Cr]_T}{1 + [H^+]/K_S}}\right)}{1 + \dfrac{[H^+]}{K_H} + \sqrt[3]{\dfrac{K_{M1}[Cr]_T}{1 + K_S/[H^+]}} + \sqrt[2]{\dfrac{K_{M2}[Cr]_T}{1 + [H^+]/K_S}}} \quad (14)$$

If the chromium hydrolysis in the solution phase is not considered, the model can be simplified by substituting K_S and K_{M2} with zero, as follows:

$$q = \frac{(b_T/3)\sqrt[3]{K_{M1}[Cr]_T}}{1 + [H^+]/K_H + \sqrt[3]{K_{M1}[Cr]_T}} \quad (15)$$

The biosorption model contains two metal binding constants (K_{M1} and K_{M2}) to be estimated. For the parameter estimation, the model was fitted to the isotherms experimentally obtained at various pH values using the Marquardt–Levenberg algorithm (15). The estimated parameters are summarized in Table 3 for both cases with and without

TABLE 3. Chromium Binding Constants[a]

With Considering Chromium Hydrolysis Reactions
$K_{M1} = 179.5\ (1.6)$ L/mmol
$K_{M2} = 9.6\ (1.3)$ L/mmol
$R^2 = 0.98^b$

Without Considering Chromium Hydrolysis Reactions
$K_{M1} = 771.6\ (2.4)$ L/mmol
$R^2 = 0.95$

[a] Standard errors are given in parentheses. [b] The R^2 values are the coefficients of determination.
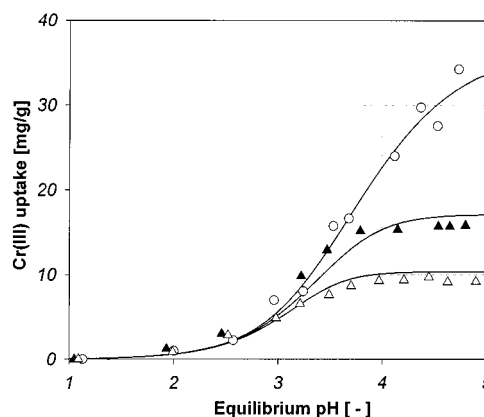
FIGURE 6. Chromium uptake by *Ecklonia* biomass as a function of the solution pH at different biomass concentrations. Biomass concentrations were (○) 1, (▲) 3, and (△) 5 g/L. The lines were produced by using the developed model (eq 14).

considering the chromium hydrolysis in the aquatic phase.

As can be seen in Figure 4, while the hydrolysis-based model can describe the isotherm experiments for all the pH values, the model not considering the hydrolysis of chromium underestimates the uptake especially at higher pH values. At pH 4, $CrOH^{2+}$ is predominant (~74%) over Cr^{3+}. Therefore, 3 mol of binding sites would not be needed to bind 1 mol of chromium. This case demonstrates the need for incorporating the metal speciation into the biosorption model—particularly for cases where metal hydrolysis strongly depends on the pH and the metal concentration.

The developed model (eq 14) was applied in an attempt to predict the "pH edge" experimental data (Figure 6) obtained at different biomass concentrations. As expected, the higher the solution pH, the higher the metal uptake. The chromium uptake (q) decreased with increasing biomass concentration because the final chromium concentration remained at trace levels. To predict the pH edge data, the chromium concentrations in the equilibrium state should be known. Although the chromium concentration of each flask was measured at the equilibrium state, the concentrations between the discrete data points could not be known. Therefore, in this study, the biosorption model was simultaneously solved with chromium mass balance equation (eq 1) expressing a relationship among the metal uptake, initial, and final (in the equilibrium state) chromium concentrations. The developed model was able to successfully predict the sorption edge behavior as a function of equilibrium pH and the biomass concentration, thus confirming the model validity. It should be noted that the present model (eq 14) does not take into account the ionic strength and thereby electrostatic effects. For a more reliable prediction of the performance of chromium biosorption in systems that involve a high level of ionic impurities, a further development of the present model would be required.

Speciation of Binding Sites. The speciation of binding sites as a function of the solution pH was simulated using
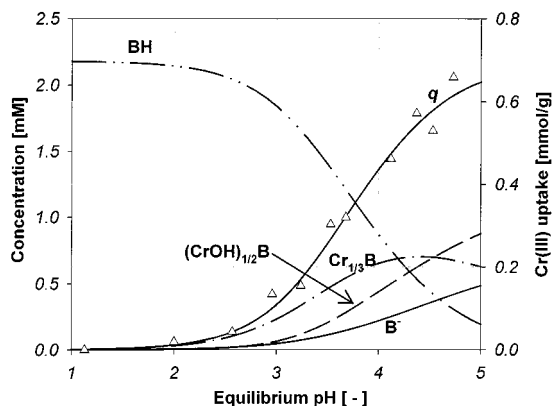
FIGURE 7. Speciation of binding sites as a function of the solution pH. The lines were produced by the developed model (eq 14). The initial chromium concentration and the biomass concentration were 1 mM and 1 g/L, respectively.

the biosorption model. As can be seen in Figure 7, below pH 2.0 almost all of the binding sites were occupied by protons, and the metal binding could not be expected. As the pH increased, Cr^{3+} species began to bind to the functional groups, and the maximum binding of this species occurred at pH 4.3. At lower pH, the $CrOH^{2+}$ binding remained at a level lower than that of Cr^{3+}. However, it gradually increased with the pH, eventually exceeding the level of Cr^{3+} binding at pH > 4.5. While the concentrations of Cr^{3+} and $CrOH^{2+}$ in the aqueous phase were identical at pH 3.55, the uptakes of the two species were the same at pH 4.5. The contribution of Cr^{3+} binding to the chromium uptake was significant even at pH > 3.55. This indicates the fact that the affinity of Cr^{3+} to the binding sites is likely to be much larger than that of $CrOH^{2+}$, which can be also confirmed from the binding constants of Cr^{3+} and $CrOH^{2+}$ (Table 3). As shown in Figure 7, the empty sites (B^-) are present especially at a high pH (>3), which can further bind the chromium ion species if higher final concentration of chromium would be used.

Acknowledgments

Glossary

[ ]	representative of concentration for bracketed species (mg/L or mmol/L)
$[\ ]_i$, $[\ ]_f$, $[\ ]_T$	initial, final, or total concentration of bracketed species (mg/L or mmol/L)
B	representative of the functional group in the biomass
b_T	amount of functional group per unit mass of biomass (mmol/g)
K_H	dissociation constant of functional group as defined in eq 2 (mol/L)
K_{M1}	binding constant of Cr^{3+} to functional group (L/mol)
K_{M2}	binding constant of $CrOH^{2+}$ to functional group (L/mol)
K_S	hydrolysis constant of chromium as defined in eq 7 (mol/L)
q	uptake of chromium on biomass (mg/g)
V	solution volume (L)
W	dry weight of biomass (g)
X	concentration of biomass (g/L)

Literature Cited

(1) Manahan, S. E. *Environmental Chemistry*, 5th ed.; Lewis Publishers: Chelsea, MI, 1991.

(2) Evangelou, V. P. *Environmental Soil and Water Chemistry: Principles and Applications*; John Wiley & Sons: New York, 1998; pp 476−498.

(3) Eisler, R. *Chromium Hazards to Fish, Wildlife, and Invertebrates: A Synoptic Review*; Biological Report 85 1.6; Contaminated Hazard Reviews Report 6; U.S. Department of the Interior, Fish and Wildlife Service: Laurel, MD, 1986.

(4) Kratochvil, D.; Pimentel, P.; Volesky, B. *Environ. Sci. Technol.* **1998**, *32*, 2693−2698.

(5) Solisio, C.; Lodi, A.; Converti, A.; Del Borghi, M. *Water Res.* **2000**, *34*, 3171−3178.

(6) Ferraz, A. I.; Teixeira, J. A. *Bioprocess Eng.* **1999**, *21*, 431−437.

(7) Dean, S. A.; Tobin, J. M. *Resour. Conserv. Recycl.* **1999**, *27*, 151−156.

(8) Madrid, Y.; Barrio-Gordoba, M. E.; Camara, C. *Analyst* **1998**, *123*, 1593−1598.

(9) Tobin, J. M.; Roux, J. C. *Water Res.* **1998**, *32*, 1407−1416.

(10) Low, K. S.; Lee, C. K.; Tan, S. G. *Environ. Sci. Technol.* **1997**, *18*, 449−454.

(11) Yun, Y.-S.; Lim, H. S.; Park, J. J.; Park, D.; Park, J. M.; Volesky, B. *Water Res.*, submitted for publication.

(12) Fourest, E.; Volesky, B. *Appl. Biochem. Biotechnol.* **1997**, *67*, 33−44.

(13) Volesky, B. In *Biosorption of Heavy Metals*; Volesky, B., Ed.; CRC Press: Boca Raton, FL, 1990; pp 7−43.

(14) Clesceri, L. S.; Greenberg, A. E.; Eaton, A. D. *Standard Methods for the Examination of Water and Wastewater*, 20th ed.; American Public Health Association, American Water Work Association, and Water Environment Federation: Washington, DC, 1998; pp 366−368.

(15) Mardquardt, D. W. *J. Soc. Ind. Appl. Math.* **1963**, *11*, 431−441.

(16) Wolfram, S. *The Mathematica Book*, 3rd ed.; Wolfram Research: Champaign, IL, 1996.

(17) Hunt, S. In *Immobilization of Ions by Biosorption*; Eccles, H., Hunt, S., Eds.; Ellis Horwood: Chichester, 1986; pp 15−46.

(18) Schiewer, S.; Volesky, B. *Environ. Sci. Technol.* **1997**, *31*, 1863−1871.

(19) Segel, I. H. *Biochemical Calculations*, 2nd ed.; Wiley: New York, 1976.

(20) Vien-Lin, D.; Colthup, N. B.; Fateley, W. G.; Grasselli, J. C. *The Handbook of Infrared and Raman Characteristic Frequencies of Organic Molecules*; Academic Press: San Diego, 1991.

(21) Kapoor, A.; Viraraghavan, T. *Bioresour. Technol.* **1997**, *61*, 221−227.

(22) Fourest, E.; Volesky, B. *Environ. Sci. Technol.* **1996**, *30*, 277−282.

(23) Pagnanelli, F.; Petrangeli-Papini, M.; Toro, L.; Trifoni, M.; Veglio, F. *Environ. Sci. Technol.* **2000**, *34*, 2773−2778.

(24) Figueira, M. M.; Volesky, B.; Mathieu, H. J. *Environ. Sci. Technol.* **1999**, *33*, 1840−1846.

(25) Yang, J. B.; Volesky, B. *Environ. Sci. Technol.* **1999**, *33*, 4079−4085.

(26) Rai, D.; Sass, B. M.; Moore, D. A. *Inorg. Chem.* **1987**, *26*, 345−349.

(27) Haug, A.; Smidsrod, O. *Acta Chem. Scand.* **1970**, *24*, 843−854.

(28) Crist, R. H.; Martin, J. R.; Guptill, P. W.; Eslinger, J. M.; Crist, D. R. *Environ. Sci. Technol.* **1990**, *24*, 337−342.

(29) Schiewer, S.; Volesky, B. *Environ. Sci. Technol.* **1995**, *29*, 3049−3058.

(30) Buffle, J. *Complexation Reactions in Aquatic Systems: An Analytical Approach*; Ellis Horwood: Chichester, 1988; pp 156−157, 280−283, 323.